Biochemical Pharmacology, Vol. 52, pp. 1103–1111, 1996.

ISSN 0006-2952/96/$15.00 + 0.00
PII S0006-2952(96)00457-1

Conversion of Irinotecan (CPT-11) to Its Active Metabolite, 7-Ethyl-10-hydroxycamptothecin (SN-38), by Human Liver Carboxylesterase

Laurent P. Rivory, Mark R. Bowles, Jacques Robert† and Susan M. Pond*
UNIVERSITY OF QUEENSLAND DEPARTMENT OF MEDICINE, PRINCESS ALEXANDRA HOSPITAL, BRISBANE, QUEENSLAND, 4102, AUSTRALIA; AND †INSTITUT BERGONIÉ, BORDEAUX CEDEX 33076, FRANCE

ABSTRACT. We have investigated the conversion of the novel anti-topoisomerase I agent CPT-11 (irinotecan; 7-ethyl-10[4-(1-piperidino)-1-piperidino]carbonyloxycamptothecin) to its active metabolite, SN-38 (7-ethyl-10-hydroxycamptothecin), by human liver carboxylesterase (HLC). Production of SN-38 was relatively inefficient and was enzyme deacylation rate-limited with a steady-state phase occurring after 15–20 min of incubation. This later phase followed Michaelis–Menten kinetics with an apparent K_m of 52.9 ± 5.9 μM and a specific activity of 200 ± 10 μmol/sec/mol. However, the total enzyme concentration estimated from the intercept concentrations of SN-38 was much lower than that estimated directly from the titration of active sites with paraoxon (0.65 vs. 2.0 μM, respectively). Because deacylation rate-limiting kinetics result in the accumulation of inactive acyl–enzyme complex, we postulated that incubation of CPT-11 with HLC would result in an inhibition of the HLC-catalysed hydrolysis of *p*-nitrophenylacetate (p-NPA), an excellent substrate for this enzyme. Indeed, this was found to be the case although complete inhibition could not be attained. Analysis of possible kinetic schemes revealed that the most likely explanation for the disparity in estimated enzyme concentrations and the incomplete inhibition of p-NPA hydrolysis is that CPT-11 also interacts at a modulator site on the enzyme, which profoundly reduces substrate hydrolysis. Furthermore, loperamide, a drug often used for the treatment of CPT-11-associated diarrhea, was found to inhibit both CPT-11 and p-NPA HLC-catalysed hydrolysis, most likely by a similar interaction. These observations have direct implications for the clinical use of CPT-11. BIOCHEM PHARMACOL 52;7:1103–1111, 1996.

KEY WORDS. camptothecin; irinotecan; enzyme kinetics; carboxylesterase (EC 3.1.1.1); loperamide

CPT-11‡ is a novel and water-soluble analogue of 20(S)-camptothecin [1]. CPT-11 displays encouraging activity in the treatment of several types of tumours including non-small cell lung cancer, colorectal adenocarcinoma, and cancer of the cervix [2]. SN-38, an important metabolite of CPT-11, has been shown to be 100–1000 times more potent than CPT-11 in *in vitro* and *in vivo* tests of cytotoxicity, inhibition of tumour growth, and interaction with topoisomerase I, the presumed target of the camptothecin family of compounds [3]. Therefore, CPT-11 is widely considered to be a pro-drug of SN-38. Conversion of CPT-11 to SN-38, however, is modest, and, at the doses used in phase II trials (>300 mg/m^2), most of the drug is excreted as unchanged CPT-11 [4]. Furthermore, the plasma concentrations of SN-38 are usually one to two orders of magnitude lower than those of CPT-11 [4]. The biotransformation of CPT-11 *in vivo* is mediated by carboxylesterases [5] and a rat serum CPT-11 carboxylesterase has been purified and characterized [6]. Detailed analysis of the hydrolysis of CPT-11 by the rat serum enzyme has revealed deacylation rate-limiting kinetics characterized by an initial rapid release of SN-38 followed by a much slower steady-state rate. A comparison of liver carboxylesterases from several species has shown that the human enzyme is among the least efficient at catalysing the biotransformation of CPT-11 to SN-38 [5], which may explain the modest conversion of CPT-11 to SN-38 observed in patients.

In this study, we have investigated the hydrolysis of CPT-11 by purified HLC in an attempt to understand the comparatively low activity of this enzyme. This reaction was also probed with studies of the interaction of CPT-11 and the carboxylesterase substrate p-NPA.

MATERIALS AND METHODS

Chemicals

CPT-11 and SN-38, prepared by Yakult (Tokyo, Japan), were provided by Rhone–Poulenc Rorer (Neuilly, France).

* Corresponding author: Dr. Laurent P. Rivory, University of Queensland, Department of Medicine, Princess Alexandra Hospital, Ipswich Road, Woolloongabba, 4102, Queensland, Australia. Tel. 61-7-3240-2839; FAX 61-7-3240-5399.

‡ *Abbreviations:* CPT-11, irinotecan (7-ethyl-10[4-(1-piperidino)-1-piperidino]carbonyloxycamptothecin); SN-38, 7-ethyl-10-hydroxycamptothecin; HLC, human liver carboxylesterase; p-NPA, *p*-nitrophenylacetate; and p-NP, *p*-nitrophenol.

Received 21 December 1995; accepted 23 April 1996.

p-NPA, p-NP, paraoxon (diethyl *p*-nitrophenyl phosphate) and loperamide (4-[*p*-chlorophenyl]-4-hydroxy-*N*,*N*-dimethyl-α,α-diphenyl-1-piperidinebutyramide) HCl were purchased from the Sigma Chemical Co. (St. Louis, MO, U.S.A.). Paraoxon was purified by passing a chloroform solution through a column of neutral alumina (activity grade I, Sigma), and then removing the chloroform by evaporation. All other reagents were of analytical grade or above. Stock solutions of loperamide (50 mg/mL) were prepared in acetonitrile/water (50:50, v/v) and stored at 4°.

Carboxylesterase

HLC (EC 3.1.1.1, mid pI isozyme) was purified as per Ketterman *et al.* [7]. Following the final purification step, preparative isoelectric focussing, the enzyme was recovered in PBS at a concentration of approximately 2 mg/mL. The enzyme, which represents the bulk of the p-NPA-hydrolysing activity of human liver [7], was stored at −70° until required. The concentration of the active enzyme was estimated by the direct titration of active sites essentially according to the method of Horgan *et al.* [8]. Briefly, the release of p-NP was measured following the addition of 50 μL of the enzyme preparation to 800 μL of paraoxon in PBS (final concentration = 54.4 μM) after first correcting for any free p-NP. This experiment was carried out with a Cary 4E spectrophotometer (Varian Australia Pty Ltd., Brisbane, Australia) at room temperature. The molar extinction coefficient (ε) of p-NP in the same conditions was determined to be 13,520 $M^{-1}cm^{-1}$.

HPLC

The concentrations of total SN-38 produced during the incubation of CPT-11 with HLC were measured by HPLC using a modification of Rivory and Robert [9]. Briefly, separation was carried out using a C-18 NovaPak RadialPak column (3 × 25 mm, Waters, Millipore Corp., Milford, MA, U.S.A.), preceded by the corresponding GuardPak guard column (Waters), at ambient temperature and with a solvent flow of 1.5 mL/min. Peak detection was performed with a Waters 470 fluorimeter (Waters) with excitation and emission wavelengths biased towards SN-38 detection at 380 and 540 nm, respectively. The mobile phase consisted of 23% (v/v) acetonitrile and 77% (v/v) 0.075 M ammonium acetate buffer (pH 5.3). The retention times were 3 and 4 min, respectively, for CPT-11 and SN-38, allowing rapid sample analysis. Samples were loaded into disposable mini-vials just prior to analysis, and 20 μL was injected by a WISP automatic injector (Waters). Data were collected and analysed using Maxima software (Waters). Standard samples were prepared from a 1 mg/mL stock solution of SN-38 in DMSO diluted serially into PBS. Standard curves were constructed for each batch of samples and were linear over the range of interest (0.1 to 10 μM, $r > 0.99$).

Hydrolysis of CPT-11

Incubations of HLC with CPT-11 were carried out in PBS at 37° in mini Eppendorf tubes (Sarstedt, Germany). A stock solution of CPT-11 (100 mg/mL) was prepared directly in PBS, and the pH was corrected to pH 7.4. An aliquot of the enzyme stock (10 μL) was added to 70 μL of PBS. Following 5 min of equilibration at 37°, the reaction was initiated by the addition of the required dilution of the CPT-11 stock (20 μL) to yield concentrations of CPT-11 ranging from 8 to 150 μM in a total of 100 μL (1/10 dilution of stock HLC). The tubes were agitated in a shaking water bath maintained at 37°. Aliquot samples (20 μL) were withdrawn at regular intervals and mixed immediately with 50 μL of an ice-cold mixture of acetonitrile, water and 0.1 N HCl (33:33:33, by vol.) and assayed for total SN-38 as detailed above. To test inhibition by loperamide, it was added to the reaction mixture prior to the additions of enzyme and CPT-11.

Hydrolysis of p-NPA

The enzymatic hydrolysis of p-NPA was followed spectrophotometrically at 400 nm [7] in a Uvikon 810 spectrophotometer (Kontron, Schlieren, Switzerland) equipped with a thermostatic cuvette holder. Reactions were carried out in 2 mL PBS (pH 7.4) at 37° in disposable acrylic cuvettes (Sarstedt, Nümbrecht, Germany). The order of addition of the reactants varied depending on the experiment. Normally, p-NPA was added to the PBS, and the spontaneous rate of hydrolysis was recorded prior to the addition of an aliquot (5 μL) of a 1:10 dilution of the enzyme stock. The measured initial rate of p-NP release was corrected for the observed spontaneous rate of hydrolysis. In the CPT-11 preincubation experiments, the enzyme was added to the PBS containing the required CPT-11 concentration, and the p-NPA was added only after the desired period of incubation. In this case, the spontaneous rate of hydrolysis was measured independently in parallel experiments. The extinction coefficient of p-NP, estimated under identical conditions as being 13,820 $M^{-1}cm^{-1}$, was used to calculate the enzyme-catalysed rate of hydrolysis. Absorbance of the buffer was monitored prior to the addition of p-NPA and enzyme to exclude significant baseline shift due to interference by CPT-11 or loperamide in the inhibition studies.

Statistics and Kinetic Modelling

All experiments were performed at least in triplicate. Michaelis–Menten and other postulated schemes of enzyme kinetics were fitted to the data obtained by non-linear least-squares regression (SigmaPlot, Jandel Scientific, Corte Madera, CA, U.S.A.) using the inverse of the observed standard deviation as weighting. Double-reciprocal plots were used for graphical purposes only. Values reported are means ± standard deviation.

RESULTS

Carboxylesterase

The release of p-NP observed during the titration of HLC with paraoxon was extremely rapid and attained an equilibrium value after only a few seconds. The resulting absorbance corresponded to a concentration of active enzyme of 20.3 μM.

Hydrolysis of CPT-11 by HLC

The production of SN-38 from 100 μM CPT-11 over a 2-hr incubation with HLC is shown in Fig. 1. As can be seen, there was an initial rapid biotransformation that slowed down to reach a steady-state velocity after approximately 20 min. A linear regression of the concentration versus time plot from 30 min onwards yielded a steady-state velocity and a significant Y-axis intercept. The same time points (30, 60, 90, and 120 min) were used to determine steady-state kinetics for a range of CPT-11 concentrations ranging from 8.8 to 146 μM. All regressions yielded $r > 0.99$ (Fig. 2). The velocities and intercepts are shown as a function of CPT-11 concentration in Figs. 3 and 4, respectively. The intercept concentrations were corrected for a small contamination of the CPT-11 by SN-38. Spontaneous hydrolysis of CPT-11 in the absence of the enzyme could not be detected over the time scale of the incubations.

The velocity (v) and intercept (τ) predicted from Scheme I in Fig. 5 are [10]:

$$v = \frac{k_3 E_t C}{K'_m + C} = \frac{V_{max} C}{K'_m + C} \quad (1)$$

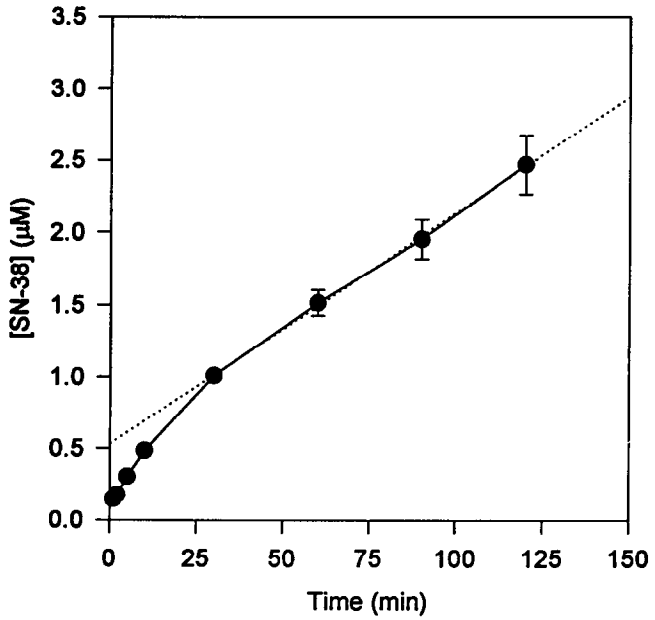

FIG. 1. Production of SN-38 during the incubation of HLC with CPT-11 (100 μM). The rapid early phase slowed down to reach a steady-state rate. Linear regression (dotted line) of the later phase yielded a steady-state velocity and an intercept concentration of SN-38. Data are means ± SD, N = 3.

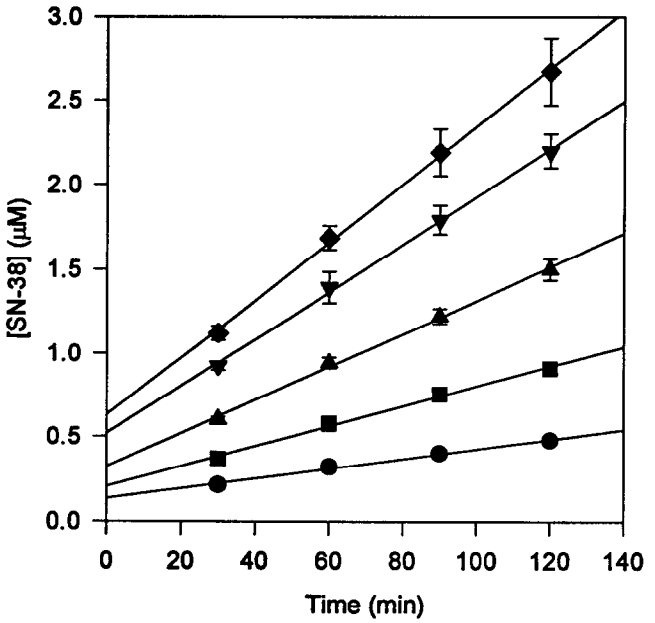

FIG. 2. Steady-state production of SN-38 during the incubation of HLC with a range of CPT-11 concentrations (circle, 8.8; square, 18; triangle, 36; inverted triangle, 74; and diamond, 146 μM). Data are means ± SD, N = 3.

and

$$\tau = \frac{E_t}{\left(1 + \frac{K'_m}{C}\right)^2} \quad (2)$$

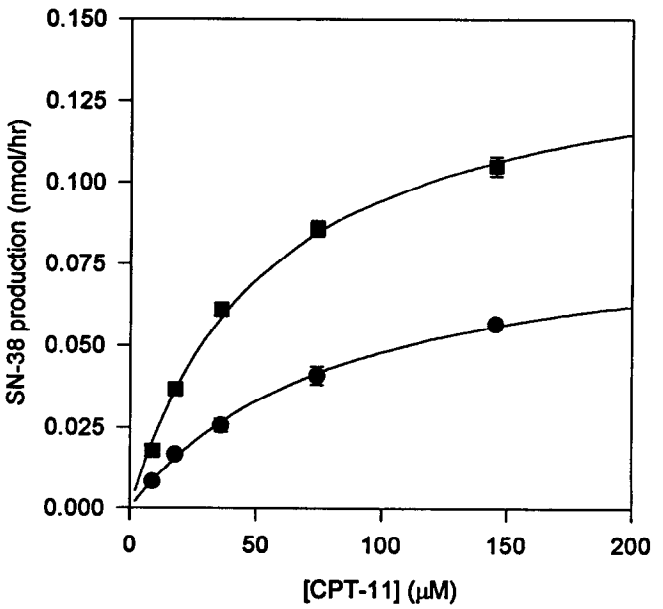

FIG. 3. Steady-state rate of production of SN-38 from CPT-11 in the presence (circle) and absence (square) of loperamide at a concentration of 50 μM. The solid lines represent the best fit of the Michaelis–Menten equation (Equation 1). Data are means ± SD, N = 3.

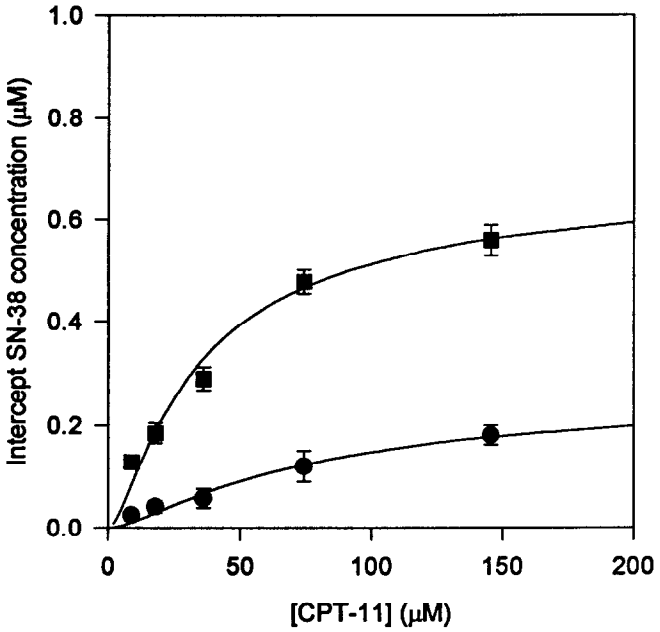

FIG. 4. Intercept concentration of SN-38 following the incubation of CPT-11 with HLC in the presence (circle) and absence of (square) of loperamide at a concentration of 50 μM. The solid lines represent the best fit of the intercept equation (Equation 2). Data are means ± SD, N = 3.

respectively, where E_t and C are the total enzyme and CPT-11 concentrations, respectively. K'_m, the apparent Michaelis-Menten constant, is defined as [10]:

$$\frac{(k_{-1} + k_2)k_3}{k_1 k_2} \qquad (3)$$

Fitting of Equations 1 and 2 to the data presented in Figs. 3 and 4 yielded estimates of V_{max} and K'_m of 0.145 ± 0.008 nmol/hr and 52.9 ± 5.9 μM, respectively, from the velocity data, and 0.67 ± 0.07 and 15.2 ± 3.2 μM for E_t and K'_m, respectively, from the intercept data. There was no obvious reason for the disparity in K'_m between the two data sets except that the intercept is an extrapolated value and may be subject to bias, particularly when the reaction velocity is low.

Inhibition of the HLC-Catalysed Hydrolysis of p-NPA by CPT-11

Deacylation-limited kinetics occur when $k_3 \ll k_2$ and result in the accumulation of the acyl–enzyme complex (EA in Scheme I of Fig. 5). Because the kinetics presented in Fig. 1 are compatible with the accumulation of EA during the hydrolysis of CPT-11 by HLC, we investigated the effect of preincubation of HLC with CPT-11 (300 μM) on p-PNA hydrolysis (1 mM). As can be seen from Fig. 6A, there was a decline in the rate of p-PNA hydrolysis with time of incubation. The control (no CPT-11) experiments also showed some decrease. This is likely to be the consequence of the extreme dilution of the enzyme because incubations

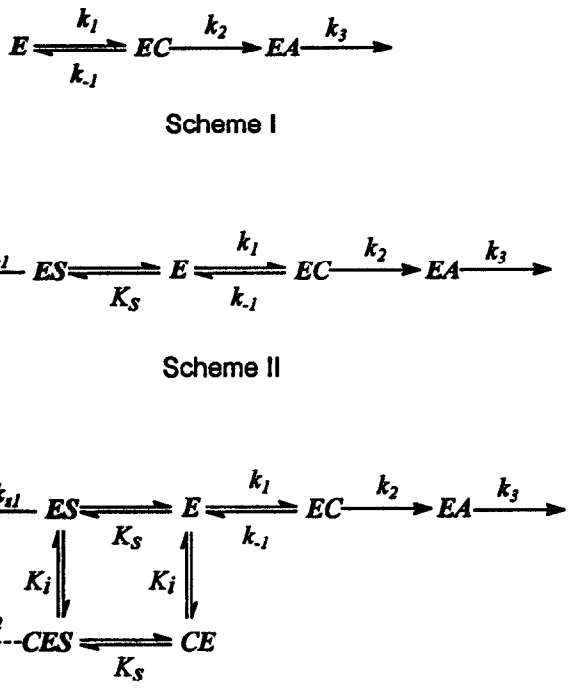

FIG. 5. Kinetic schemes for: (I) the deacylation rate-limited hydrolysis of CPT-11; (II) the competitive inhibition of p-NPA hydrolysis by CPT-11; (III) the inhibition of p-NPA hydrolysis by CPT-11 by combined competitive and non-competitive mechanisms; and (IV) the substrate modulation of CPT-11 hydrolysis by non-competitive binding. E, EC, ES and EA are free enzyme, enzyme-CPT-11 complex, enzyme-p-NPA complex, and acyl–enzyme complex, respectively. SN-38 is produced from the cleavage of EC with rate k_2. Deacylation of *EA* releases free enzyme (*E*) and bipiperidino carboxylic acid. For the other enzyme species (CES, CE and CEC), the prefix C indicates the presence of CPT-11 at the modulator site, and K_i is the equilibrium binding constant for this interaction. The rate constants k_{s1} and k_{s2} represent the cleavage of p-NPA to p-NP. In Scheme III, full non-competitive inhibition occurs when k_{s2} = 0.

of enzyme at the 400-fold higher concentration used in the CPT-11 experiments before dilution and assay with p-NPA revealed no loss in activity. Nevertheless, the loss in the controls was taken into consideration when estimating the percentage of inhibition due to CPT-11 (Fig. 6B), which appeared to reach a plateau value after approximately 15 min. There was some inhibition even when p-NPA was

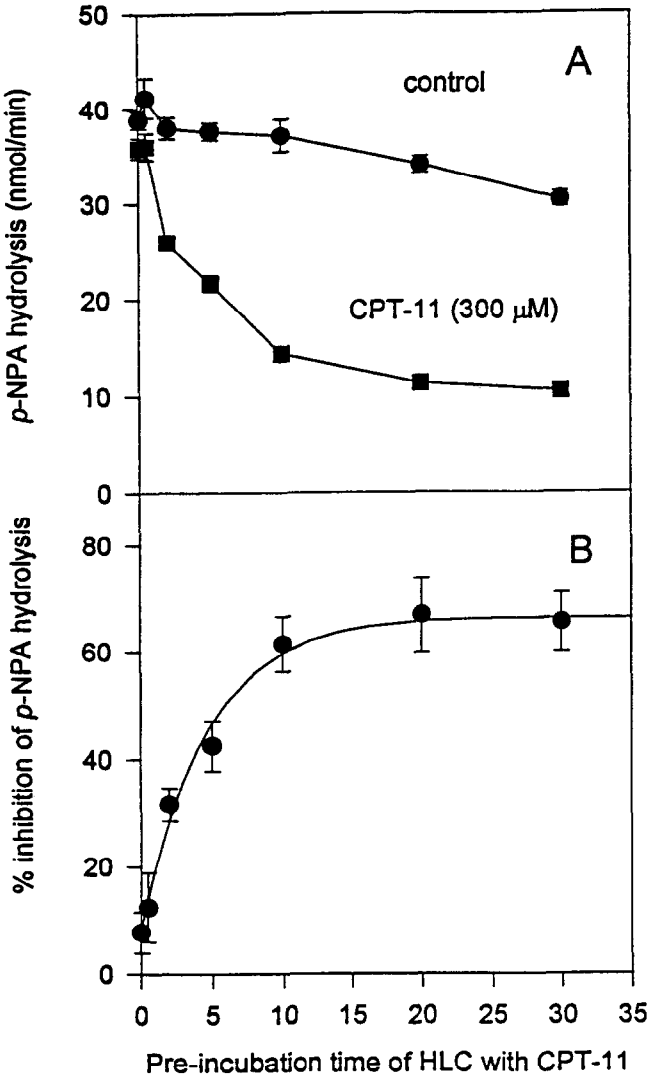

FIG. 6. Rate of hydrolysis of p-NPA in the presence and absence of 300 μM CPT-11 (A) and the relative inhibition (%) of the hydrolysis as a function of time (B). Data are means ± SD, N = 3.

added prior to the CPT-11 (zero time). The addition of SN-38 (5 μM) did not result in any significant inhibition of p-NPA hydrolysis (data not shown).

Experiments were performed to investigate the effect of CPT-11 concentration on p-NPA hydrolysis following the incubation of HLC with CPT-11 for 15 min at 37°. Because the simplest scheme of interaction which could be considered was Scheme II of Fig. 5, we used saturating concentrations of p-NPA (see below) to shift the equilibrium towards p-NPA hydrolysis. We surmised that this new equilibrium would be established rapidly, whereas the acyl–enzyme complex, which is extremely stable, would be left unaffected. The net effect, therefore, was expected to be a decrease in available active enzyme. Control experiments were also performed with no preincubation to enable the deconvolution of potential inhibitory effects other than those due to the time-dependent accumulation of acyl–enzyme complex, as follows:

$$v_{preinc} = \left(\frac{E_t - EA}{E_t}\right) \cdot v_{no\ preinc}$$
$$\therefore \frac{EA}{E_t}(\%) = \left(1 - \frac{v_{preinc}}{v_{no\ preinc}}\right) \cdot 100 \qquad (4)$$

Consistent with our observations shown in Fig. 6, prior incubation with CPT-11 resulted in significantly more inhibition of p-NPA hydrolysis (Fig. 7A). Nevertheless, there was also some rapid inhibition. The calculated percentage of *EA*, shown in Fig. 7B, reached an apparent maximum of 57%, inconsistent with Scheme I which predicts that, prior to the addition of p-NPA, the percentage of *EA* should follow the relationship:

$$\frac{EA}{E_t}(\%) = \frac{C}{K'_m + C} \cdot 100 \qquad (5)$$

and approach 100% at saturating concentrations of CPT-11.

The kinetics of p-NPA hydrolysis at a range of concentrations (0.05 to 1 mM) were investigated at a fixed concentration of CPT-11 (600 μM) without preincubation. These results are shown in Fig. 8 and in double-reciprocal format in Fig. 9. CPT-11 resulted in an appreciable reduction in the V_{max} (45.2 ± 1.1 vs 59.2 ± 2.8 nmol/min) for p-NPA hydrolysis, whereas the K_m estimates were similar (0.26 ± 0.02 vs 0.23 ± 0.03 mM). Although the double-reciprocal plot suggests mixed inhibition, the proximity of the K_m estimates indicates that CPT-11 is mostly a non-competitive inhibitor of HLC (without preincubation). This is at odds with Scheme II. Scheme III (Fig. 5) is required to satisfy the observations.

Interestingly, this type of inhibition, if extended to the kinetics of CPT-11 itself as shown in Fig. 5 (Scheme IV), would have an effect on both *EA* at steady state and the SN-38 intercept. Because the time required to attain the steady-state rate of hydrolysis of CPT-11 is relatively long (Fig. 1), k_2 is likely to be small in comparison with the other rate constants of Scheme III (except for k_3). Hence, equilibrium assumptions can be used to obtain the equation for the velocity of SN-38 formation at steady state:

$$v = \frac{C E_t k_3 \dfrac{K_i}{K_i + K'_m}}{\dfrac{C^2 k_3}{(K_i + K'_m)k_2} + C + \dfrac{K'_m K_i}{K_i + K'_m}} \qquad (6)$$

The function for the effect of CPT-11 concentration on SN-38 intercept was solved using Laplace equations describing the time course of each complex over time and the boundary condition $E(0) = E_t$. Only those terms not yielding negative exponentials (≈0 at steady state) were inverted. By using the assumption made above that k_2 is small in comparison with the other rate constants (with the notable exception of k_3), we obtained:

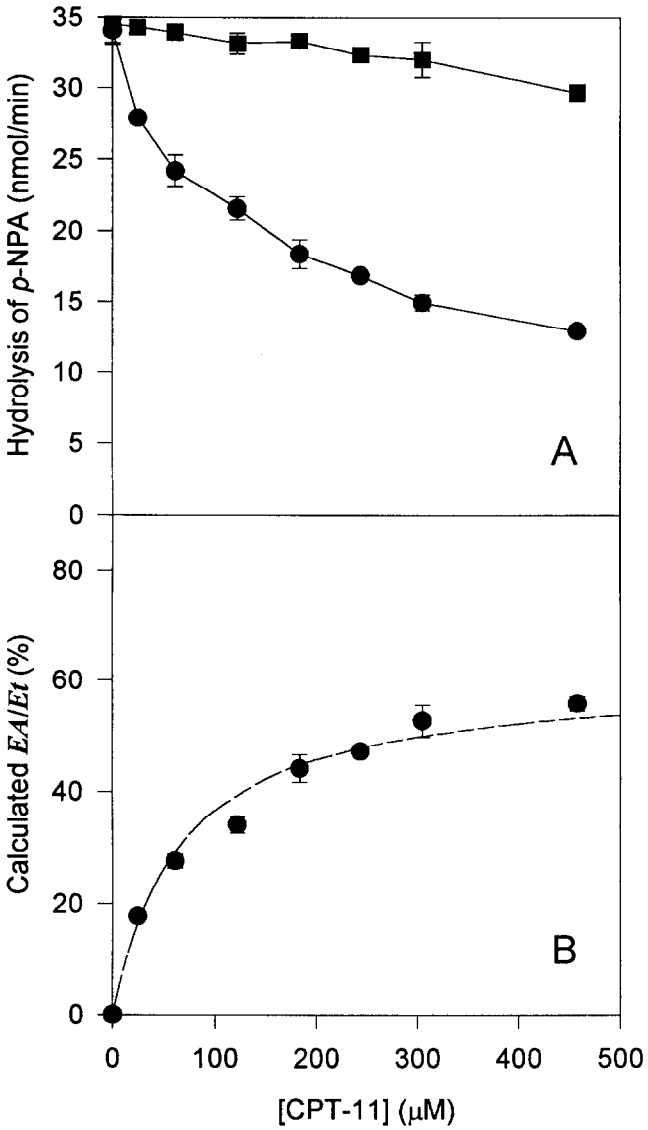

FIG. 7. (A) Rate of hydrolysis of p-NPA as a function of CPT-11 concentration following no preincubation (square) or a 15-min preincubation of HLC with CPT-11 (circle). (B) Concentration of the acyl–enzyme complex EA as a percentage of the total enzyme E_t calculated from the data shown in the top panel with Equation 4. The dashed line is the line of best fit using Equation 8. Data are means ± SD, N = 3.

$$\tau = \frac{E_t\left(\frac{K_i}{K_i + K'_m}\right)^2}{\left[\frac{C\,k_3}{(K_i + K'_m)k_2} + 1 + \frac{K'_m K_i}{(K_i + K'_m)C}\right]^2} \qquad (7)$$

It is evident that in the case where the deacylation rate is limiting ($k_3 \ll k_2$), the C^2 term in Equation 6 and, in particular, the left denominator term in Equation 7 will become negligible except when the concentrations of the substrate become large relative to the magnitude of the equilibrium constants. At lower concentrations, the result of this effect will be only minor deviations from Michaelis–

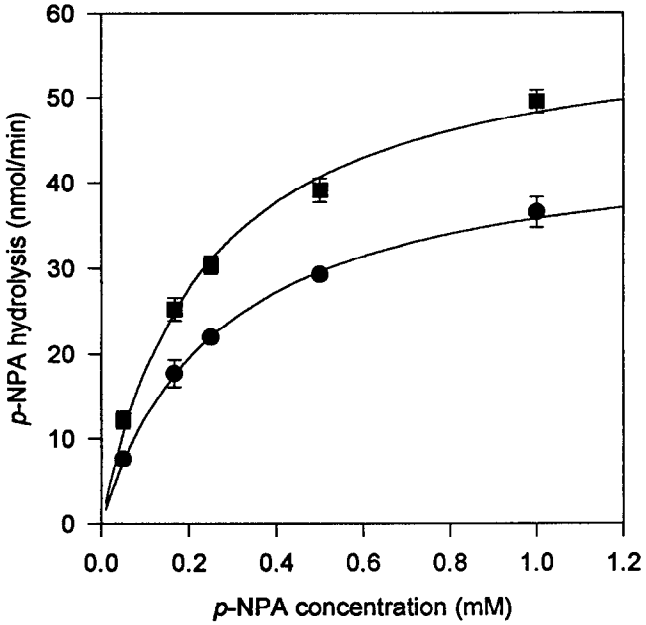

FIG. 8. Rate of p-NPA hydrolysis as a function of p-NPA concentration in the presence (circle) and absence (square) of 600 μM CPT-11 (no preincubation). Data are means ± SD, N = 3.

Menten kinetics. However, when the data are plotted in double-reciprocal format (Fig. 10), there is some apparent curvilinearity. This is consistent with the proposed scheme because at high concentrations (1/[S]→0), the velocity will start declining. One other important difference between Equation 2 and Equation 7 is that the maximum intercept will be inferior to the actual active enzyme concentration by the squared numerator term of Equation 7. Refitting the

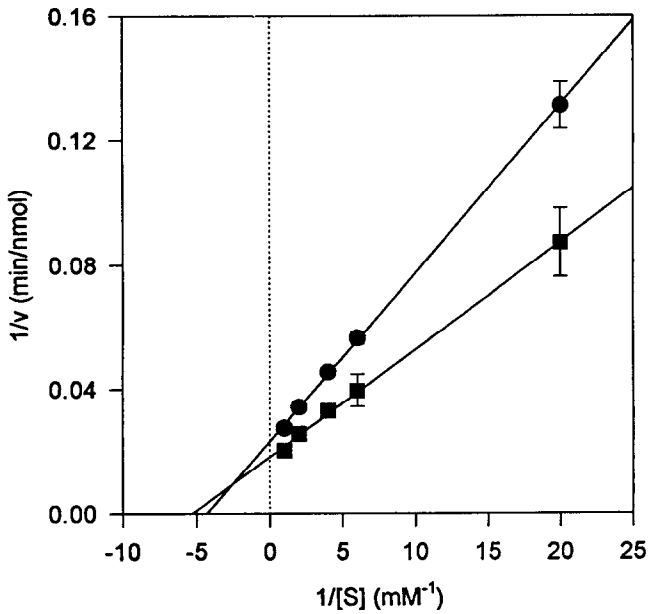

FIG. 9. Data of Fig. 8 plotted in double-reciprocal format. Solid lines are the linear regression of the data.

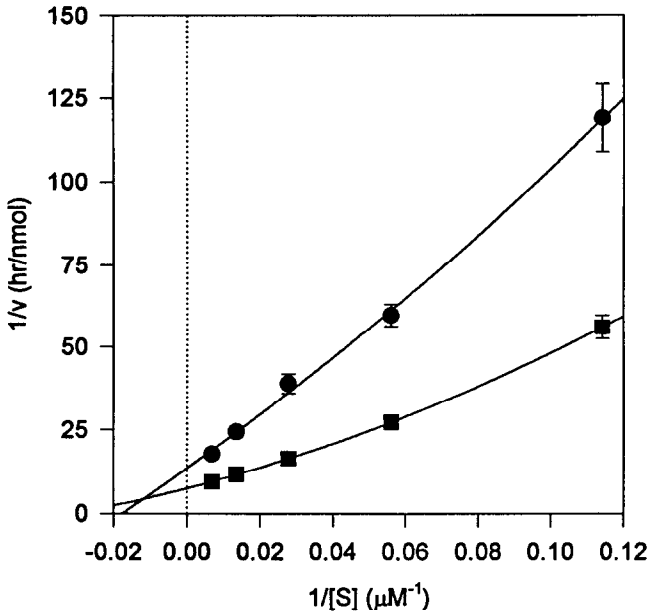

FIG. 10. Data of Fig. 3 plotted in double-reciprocal format. Note the curvilinearity of the CPT-11 data without loperamide co-incubation (square). This is much less marked in the presence of loperamide (circle).

intercept data (Fig. 4) and E_t = 2.0 μM yielded an estimate of this unitless factor, 0.59 ± 0.02.

With this model, the relative acyl–enzyme complex concentration is equal to:

$$\frac{EA}{E_t}(\%) = \frac{C\dfrac{K_i}{K'_m + K_i}}{\dfrac{C^2 k_3}{(K_i + K'_m)k_2} + C + \dfrac{K'_m K_i}{K'_m + K_i}} \cdot 100 \qquad (8)$$

and Equation 8, minus the C^2 term, was fitted to the results shown in Fig. 7. The fit shown was given with $K_i/(K_i + K'_m)$ equal to 60.8 ± 2.8%, which is in substantial agreement with that obtained from the intercept data. The term $K_iK'_m/(K_i + K'_m)$ was estimated to be 65.6 ± 8.8 μM. Although Equation 6 did provide a superior fit to that obtained with Equation 1 for the velocity data, the parameters were highly correlated with unacceptable standard deviations. Hence, the results obtained with the acyl–enzyme data were used to solve for K'_m and K_i to yield values of 107 and 167 μM, respectively. Using the equilibrium equation for fully non-competitive inhibition [11] and the ratio of the V_{max} values obtained from the fitting of the data of Fig. 8 to Michaelis–Menten kinetics in the absence and presence of 600 μM CPT-11 (59.2 ± 2.8 and 45.2 ± 1.1 nmol/min, respectively), K_i was estimated independently to be 1900 μM. This is clearly at odds with the previously determined value of 167 μM (from EA data) and suggests that the instantaneous inhibition of p-NPA hydrolysis by CPT-11 is not fully non-competitive (i.e. $k_{s2} \neq 0$). The adoption of a partially non-competitive scheme and K_i = 167 μM requires that k_{s2}/k_{s1} equal 0.69.

Inhibition of p-NPA Hydrolysis by Loperamide

Loperamide (200 μM) was found to be a more potent inhibitor of p-NPA hydrolysis than CPT-11 (no incubation). Loperamide caused a significant reduction in V_{max} (41.9 ± 1.1 vs 60.0 ± 3.1 nmol/min) and an increase in K_m (0.40 ± 0.03 vs 0.24 ± 0.03 mM), consistent with a mixed mode of inhibition (Figs. 11 and 12). Incubation of loperamide with the enzyme prior to assay did not result in a modification of this inhibition (results not shown).

Inhibition of CPT-11 Hydrolysis by Loperamide

Loperamide at 50 μM significantly reduced both the V_{max} (0.088 ± 0.004 nmol/hr, Fig. 3) of CPT-11 hydrolysis and the intercept concentrations of SN-38 (Fig. 4). The apparent K_m was increased (82.4 ± 7.4 μM). Interestingly, the presence of loperamide caused a straightening of the double-reciprocal plot (Fig. 10), suggesting that loperamide displaced CPT-11 from the modulator site.

DISCUSSION

In this study, we have investigated the hydrolysis of CPT-11 catalysed by HLC in an attempt to understand the low efficiency of conversion of this promising anti-cancer drug to its active metabolite, SN-38. Indeed, the estimated V_{max} of the steady-state conversion of CPT-11, 0.145 nmol/hr, represents an apparent enzyme turn-over time of 1.4 hr, whereas that observed for the conversion of p-NPA (V_{max} = 59.0 nmol/min), achieved with a greatly reduced quantity of enzyme, is in the vicinity of only 0.01 sec. This is equivalent to a ratio of k_{cat} values of 5 × 10^5 in favour of p-NPA

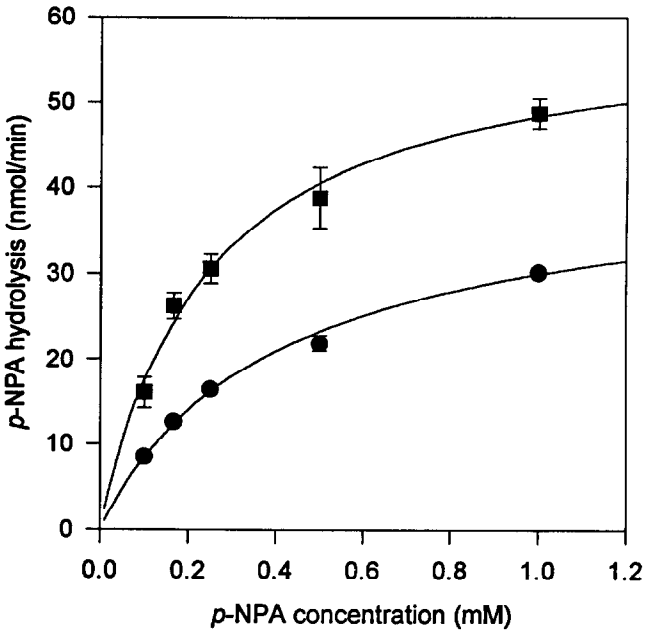

FIG. 11. Rate of p-NPA hydrolysis as a function of p-NPA concentration in the presence (circle) and absence (square) of 200 μM loperamide. Data are means ± SD, N = 3.

hydrolysis, underlying the dramatic difference in the cleavage rates of the two substrates. The fact that a steady-state rate of hydrolysis occurred following a burst release of SN-38 confirms that the cleavage of CPT-11 by carboxylesterases is deacylation-limited, as reported previously for the rat serum enzyme [6] and that the rate of deacylation is extremely slow. Nevertheless, this steady-state rate required some 10–20 min to be established, indicating that the cleavage of the substrate is also a relatively slow step. To our knowledge, there has been only one other study of CPT-11 biotransformation by purified HLC [5]. The values of K_m and V_{max} reported by Satoh *et al.* [5] were 0.169 mM and 0.161 nmol/mg/min, respectively. In their study, the reaction velocities were estimated from a single 2-min time point and, therefore, represent mostly the kinetics of the initial phase. The enzyme turn-over time can be estimated from their data (assuming molecular mass of 62 kDa [7]) to be 1.7 hr, a figure very similar to the one observed in our study. Given that we measured the slower steady-state phase, our enzyme would appear to have a greater specific activity. The difference between the K_m of the two studies can be explained by the fact that studies of the early phase will reveal a half-saturation constant somewhere between the true Michaelis–Menten constant and K'_m as given by Equation 3 [10]. Because $k_3 \ll k_2$, the constant measured by Satoh *et al.* would be expected to be substantially larger than the K'_m estimated in our study. This appears to be the case.

Although the kinetics of CPT-11 appeared to follow Michaelis–Menten kinetics (apart from some non-linearity of the double-reciprocal plot in Fig. 10), a disparity arose between the enzyme concentration estimated from the intercept kinetics and the actual active site concentration as determined by paraoxon titration. Although pure HLC is thought to exist as an equilibrium of monomer and trimer [12], it is unlikely that a masking of active sites in the trimeric form is the reason for the difference. Indeed, the kinetics of CPT-11 hydrolysis and the paraoxon titration were carried out in the same conditions and at very similar enzyme concentrations. Furthermore, the release of p-NP from paraoxon reached an equilibrium within a few seconds and remained constant thereafter, indicating the absence of a slow-dissociation phenomenon. Given the slow nature of the deacylation step, even a gradual exchange between the various forms of HLC would have resulted in the maximum concentration of enzyme being available in the CPT-11 incubations. Rather, this disparity in enzyme concentration was consistent with a scheme of non-competitive inhibition and the results obtained with both the intercept data and that obtained with the incubation-related inhibition of p-NPA hydrolysis by CPT-11 were in excellent agreement. We believe that the use of an excellent substrate of carboxylesterase to demonstrate the kinetics of the acyl–enzyme complex is a novel approach. Taken together, the two sets of results indicate that CPT-11 binds to a modulator site that reduces the efficiency of the hydrolysis of

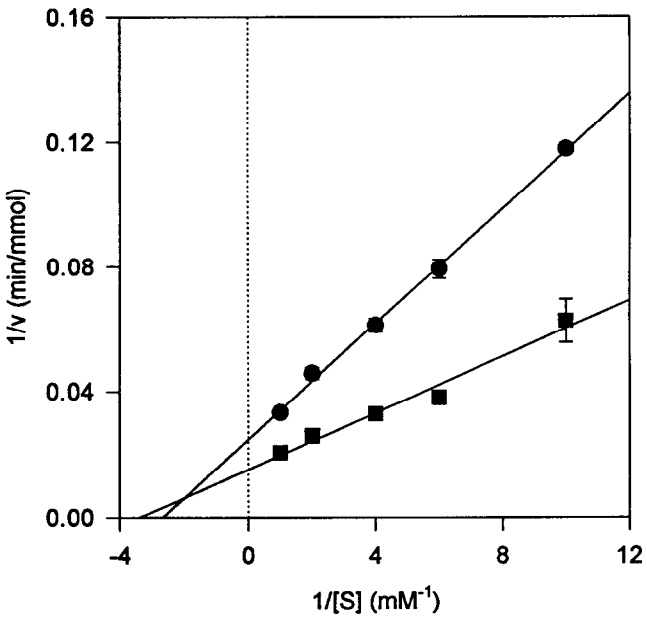

FIG. 12. Data of Fig. 11 plotted in double-reciprocal format.

CPT-11. There have been other reports of substrate modulation of hydrolysis by carboxylesterases. In the case of the study of Stoops *et al.* [13] with pig liver carboxylesterase, binding of substrate or modifier at the modulator site resulted in activation of cleavage, and the enzyme appeared to behave as two separate isozymes.

The auto-inhibition of CPT-11 hydrolysis presents a further reason for the apparent inefficiency of the biotransformation of CPT-11 by HLC. However, this is a relatively modest effect (reduction of apparent active enzyme concentration by approximately half) in comparison with the extremely slow deacylation step. Similarly, although the non-competitive interaction between CPT-11 and HLC also resulted in some inhibition of p-NPA hydrolysis, the effect was relatively minor in comparison with the reduction in enzyme activity due to the sequestration of enzyme as acyl–enzyme complex following a 15-min preincubation with CPT-11.

In a previous study[1], we correlated the rate of hydrolysis of CPT-11 (10 μM) and p-NPA (0.5 mM) by microsomes prepared from seven human livers and found that the ratio of the rates of hydrolysis of the two substrates, when corrected for protein content, was $1.6 \pm 0.4 \times 10^{-7}$. In the current study, a similar comparison of the V_{max} for the two substrates, again adjusted for enzyme content, yielded a value of 2×10^{-6}. This provides strong support for the thesis that HLC, which represents the bulk of the p-NPA hydrolytic activity [7], is also the principal CPT-11-converting enzyme of human liver.

CPT-11, like all active analogues of 20(S)-camptothecin, undergoes a reversible and pH-dependent hydrolysis from

[1] Rivory LP, Haaz M-C and Robert J, unpublished observations.

the lactone to a ring-opened carboxylate form [14]. In our study, CPT-11 was always pre-equilibrated in the identical buffer used for the enzyme incubations prior to addition to the reaction mixture to remove any effect of lactonolysis on the kinetics of CPT-11. Therefore, the kinetics reported in this study represent those of the biotransformation of CPT-11 as the mixture of its two forms as they occur *in vivo*. This does not preclude the possibility that the two forms compete for a single substrate site and/or that the rate of cleavage of the two forms could be different. We are continuing work with HLC to determine whether this is the case.

Loperamide, which is advocated at high doses for the treatment of the tardive and often debilitating diarrhea sometimes observed following CPT-11 treatment [15], was found to be an inhibitor of CPT-11 hydrolysis by HLC. However, loperamide is usually given at least 8 hr following the infusion of CPT-11 and is, therefore, unlikely to greatly influence the proportion of the dose biotransformed to SN-38. On the other hand, there was an appreciable sequestration of HLC as an inactive acyl–enzyme complex following incubation with CPT-11. This raises the possibility that CPT-11 could interfere with the metabolism of drugs that are also substrates of carboxylesterases, when administered following the CPT-11 infusion.

The authors would like to thank Dr. Peter Parsons (QIMR, Brisbane) for the loan of the Cary 4E spectrophotometer. This research was funded by a grant from the Australian National Health and Medical Research Council (NHMRC 920298). L.P.R. is the recipient of an NHMRC/INSERM Exchange Fellowship.

References

1. Sawada S, Okajima S, Aiyama R, Nokata K-I, Furuta T, Yokokura T, Sugino E, Yamaguchi K and Miyasaka T, Synthesis and antitumor activity of 20(S)-camptothecin derivatives: Carbamate-linked, water-soluble derivatives of 7-ethyl-10-hydroxycamptothecin. *Chem Pharm Bull (Tokyo)* **39:** 1446–1454, 1991.
2. Slichenmyer WJ, Rowinsky EK, Donehower RC and Kaufmann SH, The current status of camptothecin analogues as antitumor agents. *J Natl Cancer Inst* **85:** 271–291, 1993.
3. Rivory LP and Robert J, Molecular, cellular, and clinical aspects of the pharmacology of 20(S)camptothecin and its derivatives. *Pharmacol Ther* **68:** 269–296, 1995.
4. Rowinsky EK, Grochow LB, Ettinger DS, Sartorius SE, Lubejko BG, Chen T-L, Rock MK and Donehower RC, Phase I and pharmacological study of the novel topoisomerase I inhibitor 7-ethyl-10-[-4-(1-piperidino)-1-piperidino]-carbonyloxy camptothecin (CPT-11) administered as a ninety-minute infusion every 3 weeks. *Cancer Res* **54:** 427–436, 1994.
5. Satoh T, Hosokawa M, Atsumi R, Susuki W, Hakushi H and Nagai E, Metabolic activation of CPT-11, 7-ethyl-10-[4-(1-piperidino)-1-piperidino]carbonyloxy camptothecin, a novel antitumor agent, by carboxylesterase. *Biol Pharm Bull* **17:** 662–664, 1994.
6. Tsuji T, Kaneda N, Kado K, Yokokura T, Yoshimoto T and Tsuru D, CPT-11 converting enzyme from rat serum: Purification and some properties. *J Pharmacobiodyn* **14:** 341–349, 1991.
7. Ketterman AJ, Bowles MR and Pond SM, Purification and characterization of two human liver carboxylesterases. *Int J Biochem* **21:** 1303–1312, 1989.
8. Horgan DJ, Dunstone JR, Stoops JK, Webb EC and Zerner B, Carboxylesterases (EC 3.1.1). The molecular weight and equivalent weight of pig liver carboxylesterase. *Biochemistry* **8:** 2006–2013, 1969.
9. Rivory LP and Robert J, Reversed-phase high-performance liquid chromatographic method for the simultaneous quantitation of the carboxylate and lactone forms of the camptothecin derivative irinotecan, CPT-11, and its metabolite SN-38 in plasma. *J Chromatogr B Biomed Appl* **661:** 133–141, 1994.
10. Ouellet L and Stewart JA, Theory of the transient phase in an enzyme system involving two enzyme–substrate complexes. The case of the formation of products from the first complex. *Can J Chem* **37:** 737–743, 1959.
11. Dixon M and Webb EC, *Enzymes*, 3rd Edn, p. 337. Academic Press, New York, 1979.
12. Junge W, Heymann E, Krisch K and Hollandt H, Human liver carboxylesterase. Purification and molecular properties. *Arch Biochem Biophys* **165:** 749–763, 1974.
13. Stoops JK, Horgan DJ, Runnegar MTC, de Jersey J, Webb EC and Zerner B, Carboxylesterases (EC 3.1.1). Kinetic studies on carboxylesterases. *Biochemistry* **8:** 2026–2033, 1969.
14. Fassberg J and Stella VJ, A kinetic and mechanistic study of the hydrolysis of camptothecin and some analogues. *J Pharm Sci* **81:** 676–684, 1992.
15. Abigerges D, Armand JP, Chabot GG, Da Costa L, Fadel E, Cote C, Herait P and Gandia D, Irinotecan (CPT-11) high-dose escalation using intensive high-dose loperamide to control diarrhea. *J Natl Cancer Inst* **86:** 446–449, 1994.